Proceedings of Meetings on Acoustics

ICA 2013 Montreal
Montreal, Canada
2 - 7 June 2013

Musical Acoustics
Session 1pMU: Player/Instrument Coupling

1pMU7.   Time-domain simulation of the bowed cello string: Dual-polarization effect

Hossein Mansour*, Jim Woodhouse and Gary Scavone

 *Corresponding author's address: Centre for Interdisciplinary Research in Music Media and Technology, 527 Sherbrooke St. West, Montreal, H3A 1E3, Qc, Canada, hossein.mansour@mail.mcgill.ca

  A detailed time-domain simulation is implemented to model the bowed cello string. Building on earlier models, several new features have been added to make the model more realistic: in particular, both polarizations of the string motion are included, as well as the longitudinal vibrations of the bow-hair. These additional features can be turned on and off in the model to evaluate their relative importance. In all previous simulations, the bow-hair was assumed stiff enough to suppress any motion of the string perpendicular to the bowing direction. High-speed video recordings, on the contrary, have suggested that the amplitude of this motion is not negligible compared to the motion of the string in the bowing direction. The major source of this motion is tracked down to the X-Y coupling through the bridge. Although this extra dimension of vibration may not necessarily contribute much to the radiated sound by itself, it can modulate the effective bow-force, and hence affect the stick-slip motion of the string. The longitudinal vibration of the bow-hair is also included in our model. The compliance of the bow-hair was accounted for in previous studies in a crude way, but without enough detail to capture the difference between different bows.

INTRODUCTION

Time-domain simulation of the bowed string has been the subject of many studies in recent years and as a result, many features of bowed strings have been explained qualitatively and to a certain extent quantitatively [Cremer 1985, Woodhouse and Galluzzo, 2004]. Different mechanical details of the bowed string have previously been investigated in the hope of making the numerical models match the experimental measurements over a wide range of bowing gestures of musical interest. Among those details added to the model are torsional vibration of the string [Woodhouse and Loach, 1999], bending stiffness of the string [Woodhouse, 1993], effect of a close body resonance resulting in a "wolf note" [McIntyre and Woodhouse, 1979], longitudinal bow-hair compliance [Pitteroff and Woodhouse, 1998a], and the effect of the bow's finite width [Pitteroff and Woodhouse, 1998b]. This study is aimed at adding more such details to the model. More specifically, modal properties of the body, dual-polarization of the string, longitudinal vibration of the bow-hair, and the properties of the bow-stick are taking into account first separately and then all together.

The simulation results in this paper are based on modeling the best-understood musical string, a "Dominant" cello D string. For this particular string a reasonably complete set of calibration data is available, covering transverse vibration frequencies and damping factors, torsional frequencies and damping factors, and bending stiffness. In short, the characteristic impedance of the string is $Z_0=0.55$ Ns/m and a constant Q-factor of 500 is assumed and implemented in the reflection functions using the method proposed in [Woodhouse and Loach, 1999], which only reflects the intrinsic damping of the string. Torsional vibration is also taken into account and parameters were extracted from [Woodhouse and Loach, 1999]. The torsional wave has the characteristic impedance of 1.8 Ns/m, constant Q-factor of 45, and propagation speed of 1060 m/s. The reflection functions are modified as suggested in [Woodhouse, 1993], to take into account wave dispersion due to the bending stiffness of the strings. The string tension, bending stiffness, and cut off frequency were respectively 111 N, 3×10^{-4} Nm^2, and 0.3 times the Nyquist frequency. The position of the bowed point on the string is denoted by the dimensionless quantity β, which is the fractional distance of the "bow" from the bridge.

MATERIAL AND METHOD

Model of the Body

A Calibrated measurement was been made on the C-string corner of a mid-quality cello. A miniature hammer and LDV were used to make the full set of measurements in the bowing plane (i.e. *X-X, Y-Y, X-Y*, and *Y-X* where *X* represents the bowing direction and *Y* is the direction normal to that in bowing plane).

$$Y_{xx}(\omega) = \sum_k \frac{i\omega \cos^2 \theta_k}{m_k(\omega_k^2 - i\omega\omega_k/Q_k - \omega^2)} \quad Y_{yy}(\omega) = \sum_k \frac{i\omega \sin^2 \theta_k}{m_k(\omega_k^2 - i\omega\omega_k/Q_k - \omega^2)} \quad Y_{xy}(\omega) = Y_{yx}(\omega) = \sum_k \frac{i\omega \cos \theta_k \sin \theta_k}{m_k(\omega_k^2 - i\omega\omega_k/Q_k - \omega^2)} \quad \textbf{(1)}$$

Consequently, 53 modes were used to reconstruct the *X-X* admittance up to the frequency of 6 kHz. Keeping the mode frequencies and Q-factors constant, the mode amplitudes where adjusted to also reconstruct the *Y-Y* measurement, according to Eq. (1), repeated from [Woodhouse 2004]. Using the same set of modes and mode angles (θ_k), the *X-Y* admittance is reconstructed and is in relatively good agreement with the measurements.

There were two very low frequency modes (supposedly the fixture modes, below 10 Hz) which were initially put into the reconstruction functions but were ultimately removed from the body response simulation. The final result of these measurements is a set of 51 natural frequencies, Q-factors, modal mass (m), and mode angles (θ).

The body was included in the model using the IIR technique described in [Woodhouse, 2004] with few modifications. In short, one resonator was considered per each mode which is excited by the force coming from the string and modifies the reflected wave based on its velocity.

First assume that all the body modes oscillate in the bowing direction (i.e. *X* direction). If we call the incoming wave to the bridge V_{Xin}, the velocity of the bridge in bowing direction $V_{XBridge}$ and the outgoing wave V_{Xout} then:

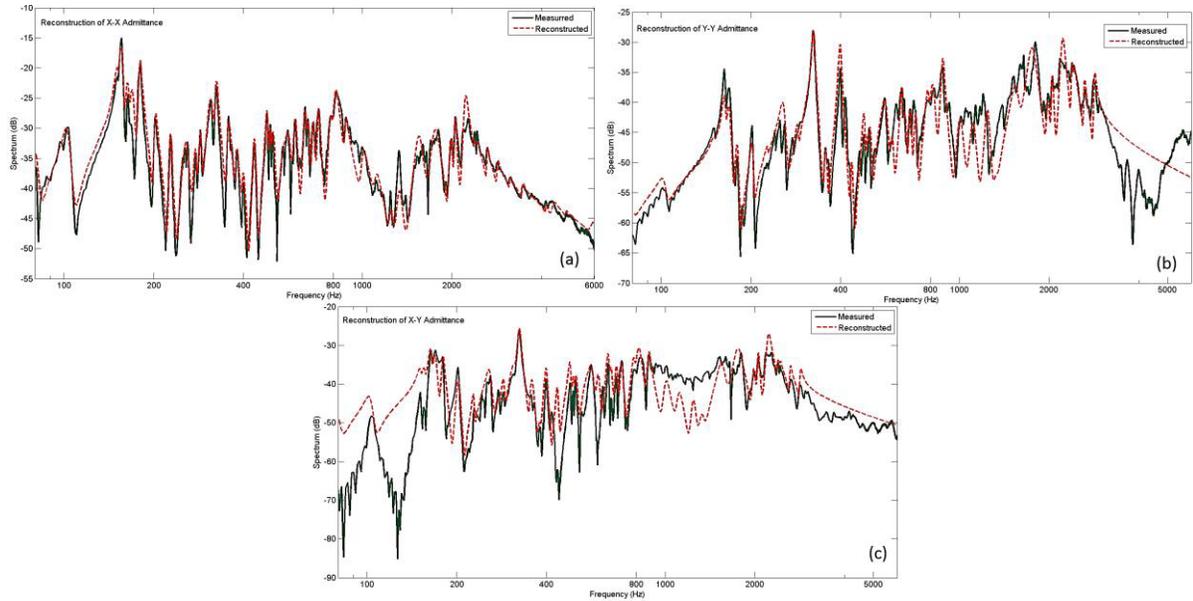$$V_{Xout} = V_{XBridge} - V_{Xin} \qquad\qquad \textbf{(2)}$$

FIGURE 1: Measured admittances on the C-string side of the cello (solid line) together with their reconstruction with 53 modes (dashed line). *X* represents bowing direction and *Y* direction is perpendicular to that. (a) *X-X* measurement, (b) *Y-Y* and (c) *X-Y* (or alternatively *Y-X*)

On the other side of the bridge, there is the afterlength of the string which can be assumed semi-infinite (or well-damped), so there will be another velocity wave of V_{after} that goes from the bridge toward the tailpiece.

$$V_{after} = V_{XBridge} \tag{3}$$

The force applied to the bridge from the string on each side is equal to the difference of the incoming and outgoing waves on that side multiplied by the characteristic impedance of the string (i.e. Z_0)

$$F_{XExcit} = Z_0 * \left[\left(V_{Xin} - (V_{XBridge} - V_{Xin}) \right) + \left(0 - V_{XBridge} \right) \right] = 2 * Z_0 * (V_{Xin} - V_{XBridge}) \tag{4}$$

It should be noted that $V_{XBridge}$ in Eq. (4) comes from the fact that even if the string is semi-infinite from both sides and there is no incoming wave to the bridge there will still be some amount of resistance against the free vibration of the bridge.

The excitation force will modify the velocity of mode k by $F_{XExcit} * h/m_k$ in each timestep where h is the timestep. The velocity that will be added to the outgoing wave from the bridge will be the sum of the velocities from each individual mode in that timestep. Note that at this point all modes are assumed to be lined up in bowing direction or at least m_k has been calculated for the projection of mode k in the bowing direction; this constraint will be relaxed when the second polarization of the string is taken into account.

Second Polarization of the String

The movement of the bridge notch is not necessarily in the bowing direction for all body modes. Also, the bow-hair is not rigid enough to suppress all the string vibrations normal to it (as is observed in our high-speed video recordings). The one dimensional model of the body is hence modified to allow for *X-Y* coupling at the bridge notch. In short, now each mode gets excited by two incoming waves instead of one, which are both projected in the principle direction of each mode. In this case, Eq. (4) will be modified as

$$F_{Excit} = 2 * Z_0 * \left((V_{Xin} - V_{XBridge}) * \cos\theta + (V_{Yin} - V_{YBridge}) * \sin\theta \right) \tag{5}$$

where θ is the vector of mode angles (used in Eq. (1)) and V_{Yin} is the incoming wave velocity in the Y direction. $V_{XBridge}$ and $V_{YBridge}$ are the projection of the bridge notch velocity in X and Y directions and are being calculated from:

$$V_{XBridge} = real(sum(modeamp.* cos(\theta)))$$
$$V_{YBridge} = real(sum(modeamp.* sin(\theta))), \hspace{3cm} \textbf{(6)}$$

in which *modeamp* is the vector of complex velocities for each mode. $V_{XBridge}$ and $V_{YBridge}$ will be added to the outgoing waves from the bridge in the X and Y directions respectively. Note that F_{Excit} in Eq. (5) and both of the right hand terms are vectors of length 51.

The bow-hair should also be flexible to allow for this second polarization of the string. Another degree of freedom is considered for this purpose. Briefly, mass per unit length of the bow ribbon is 0.0077 kg/m, length of the hair ribbon 0.65 m and tension of 60 N for the whole ribbon [Askenfelt 1995]. A Q-factor of 20 is used for the transverse waves as estimated in [Gough, 2012]. This will result in a fundamental of 68 Hz for the bow-hair in the transverse direction. The "bow beta" (distance from the contact point to the frog divided by the full length of the hair ribbon) is arbitrarily chosen to be 0.31 which does not dynamically change during the simulation as its dynamics is assumed to be much slower than the dynamics of the string itself.

The transverse vibration of the bow-hair gets excited by the normal-to-bow vibrations of the string; hence the bow and the string are coupled at the contact point. The constraint at the contact point is that they share a common velocity and apply the same amount of force to each other in opposite directions. To find the unknown common velocity and the mutual force, the velocity of the string and the bow are first calculated in the absence of the other one. These values are called V_{Yh} and V_{bth} representing history of the string velocity in the Y direction and history of the bow velocity in the transverse direction. With simple math it can be shown that the matched velocity (V_{match}) will be equal to

$$V_{match} = \frac{V_{Yh}*Z_0 + V_{bth}*Z_{bt0}}{Z_0 + Z_{bt0}} \hspace{3cm} \textbf{(7)}$$

and the resulting fluctuating force in the contact region (F_{fluc}) will be

$$F_{fluc} = 2 * Z_0 * (V_{match} - V_{Yh}) \hspace{3cm} \textbf{(8)}$$

This force is added to the nominal value of the bow-force, supplied by the player, to give the effective bow-force. Since the bow-force is being dynamically updated for each timestep the friction curve should be re-scaled consequently.

Longitudinal Bow-hair Vibration

Bow-hair has some degree of compliance in the longitudinal direction which is being excited by the fluctuating stick-slip force between the bow and the string. The characteristic impedance of each hair strand in longitudinal direction is around 0.1 Ns/m [Askenfelt 1995] and a typical bow has approximately 175 hairs, among which only 30-40 are active and in contact with the string. In this sense the effective characteristic impedance of the hair ribbon in the longitudinal direction (called Z_{bL0}) is about 4 Ns/m. The wave speed in the longitudinal direction is about 2300 m/s [Askenfelt, 1995] and the Q-value is approximated at 10 as estimated in [Gough 2012]. In the presence of bow-hair longitudinal vibrations, the nominal bow velocity will be modulated by the relative velocity of the contact point on the bow to the bow itself. This relative velocity can be found from:

$$V_{bFluc} = V_{L\_intip} + V_{L\_infrog} + \frac{fric}{2*Z_{bL0}} \hspace{3cm} \textbf{(9)}$$

and the effective bow speed can be calculated from

$$V_{bEff} = V_b - V_{bFluc} \hspace{3cm} \textbf{(10)}$$

where *fric* is the instantaneous friction force between the bow and the string, V_b is the nominal bow speed provided by the player, and V_{L_intip} and V_{L_infrog} are the incoming longitudinal velocity waves arriving at the contact point from the tip and the frog respectively. It is noteworthy that since the friction curve is a function of bowspeed, it should be reconstructed with V_{bEff} instead of V_b.

Interestingly it was observed that Helmholtz motion could not be formed with high values of bow-force unless forward slipping of the string was allowed (i.e. slipping of the string WRT the bow in the bowing direction).

Stick Modes

In a similar way as discussed for the modeling of the body, the stick modes are taken into account using a set of resonators. Fourteen modes are considered in this case whose frequencies, modal masses, and mode angles were all extracted from [Gough, 2012]; according to the same reference, Q-factors were all assumed around 30 in the absence of player's hand and 10 in actual playing conditions. The whole flexibility of the bow-stick was lumped at the tip side as the frog was assumed much heavier and more damped by the hand of the player. Stick modes are being excited by both transverse and longitudinal waves in the hair ribbon and in turn will affect both of them. Since bow-hair does not have an after-length and the characteristic impedance is different for the longitudinal and transverse modes, the calculation of the stick mode excitation is a bit different from the one of the string-body; therefore it is defined here as:

$$F_{Stick\_Excit} = Z_{bL0} * (2 * V_{L\_intip} - V_{Lstick}) * cos\,\theta_b + Z_{bt0} * (2 * V_{t\_intip} - V_{Tstick}) * sin\,\theta_b \qquad (11)$$

θ_b is the mode angles of the stick WRT the bowing direction (longitudinal direction of the bow), V_{L_intip} and V_{t_intip} are the longitudinal and transverse velocity waves arriving at the tip, and V_{Lstick} and V_{Tstick} are the velocities of the tip in longitudinal and lateral directions.

Summary of the Model

The model of the bowed string allows for a maximum of 5 different types of motion: 1) vibration of the bowed string in the bowing direction; 2) vibration of the bowed string in the direction perpendicular to the bow; 3) torsional vibration of the string; 4) transverse vibration of the bow-hair; and 5) longitudinal vibration of the bow-hair. It also uses 65 independent resonators, 51 of which are for the body modes and the remaining 14 for the bow-stick modes.

RESULTS AND DISCUSSION

Different combinations of the above mentioned degrees of freedom are allowed and their relative importance is evaluated. Schelleng maps are calculated for each to see their effect on the playability of the cello. Schelleng calculated formulae for the maximum and minimum bow-forces between which the Helmholtz motion of the string is possible, and plotted the results in the plane of force against bowing position on a log-log scale [Schoonderwaldt *et. al.* 2008]. Each map studied in this section involves 400 time-domain simulations of 1.0 second with different combinations of Beta and Bow-force (20 values for each). Beta ranged from 0.02 to 0.2 and force ranged from 0.1 N to 2.5 N. Also the bow velocity was chosen to be 0.05 m/s in all cases. Motion of the string in the bowing direction was always initialized with a proper sawtooth wave. In all cases torsional vibration of the string and its bending stiffness were taken into account. Each time domain waveform was automatically identified using the method proposed in [Woodhouse, 2003] and modified in [Galluzzo, 2003].

The Body Effect

The first study to evaluate the model was to see how the body would modify the playability of the instrument. Figure 2 shows the simulated Schelleng diagram of a rigid body Cello (i.e. rigid termination at bridge) compared to a flexible body cello as described in the modeling section. As was expected the rigid body cello has a zero minimum bow-force and its maximum bow-force is similar to the one of a flexible-body cello.
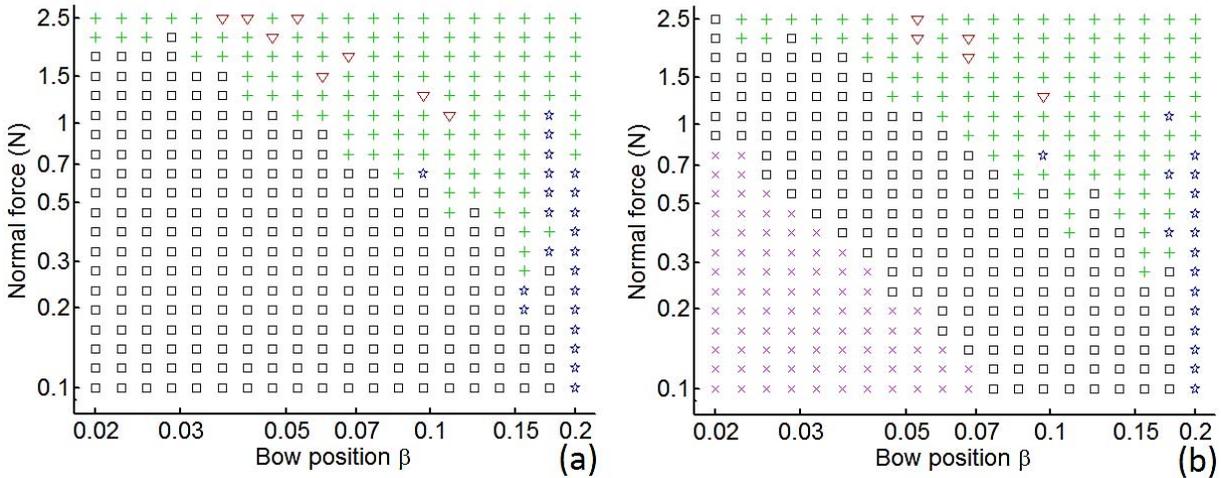
FIGURE 2: Schelleng diagram of the rigid body cello (a) compared to the one of a flexible body cello (b). 51 resonators are used to simulate the body modes. Helmholtz motion (square); multiple-slipping motion (x); aperiodic motion (+); ALF (triangle); Raman "higher type" (star).

Dual String Polarization

As described in the modeling section, adding the second polarization of the string would modulate the effective bow-force and affect the playability of the instrument. Figure 3 shows a typical response that the second polarization would create.

The set of body modes and their angles were extracted from the measurements and fed into the model. The particular case shown in Figure 3 is for Beta=0.037 and Bow-force=0.544. The blue (dash-dot) line shows the effective bow-force (F_{eff}) calculated from Eq. (13) where F_{nom} is the nominal value of Bow-force and F_{fluc} is calculated from Eq. (8)
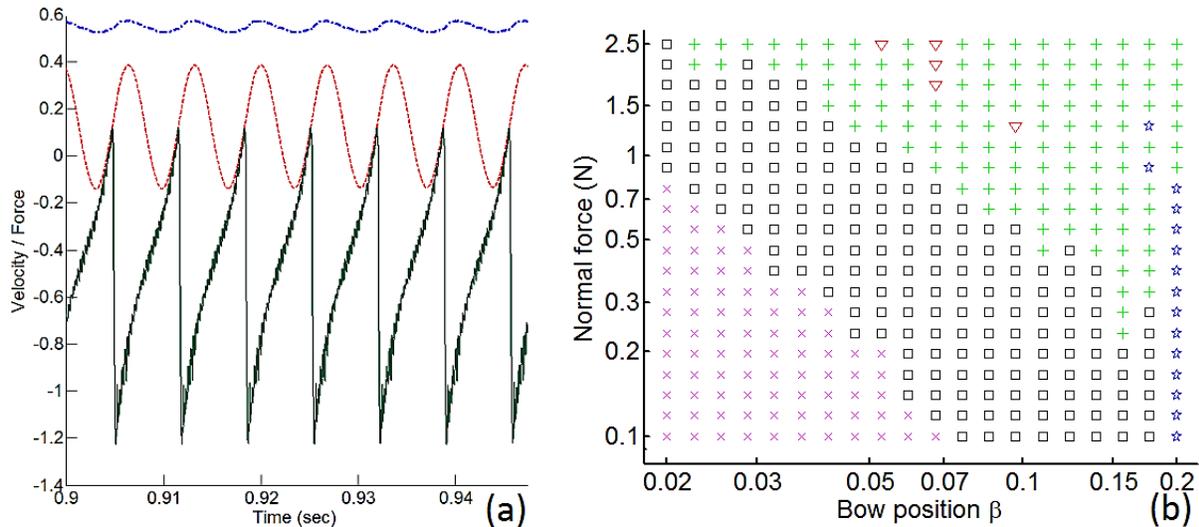
$$F_{eff} = F_{nom} + F_{fluc} \quad \textbf{(13)}$$

FIGURE 3: (a) Simulation results when the second polarization of the string was allowed, Beta=0.037 and Bow-force=0.544 N. (blue dash-dot) the effective bow-force, (red dash) velocity wave of the string perpendicular to bow and (green) velocity wave of the string in bowing direction. (b) Schelleng diagram for the bowed string with dual polarization. (left) body modes and their angles were used in the model exactly as measured

For this case the amplitude of F_{fluc} was equal to 0.03 N which is 5.5% of the nominal value. One would guess that the effect will be much larger if the string's fundamental is close to one of the instruments wolfs which in particular has an angle close to 45 degree.

An interesting observation in Figure 3 is the relatively large amplitude of perpendicular to bow vibration despite the fact that the body mode close to the string fundamental was not really suitable to excite this second polarization, otherwise one could expect an even larger amplitude for that. The Schelleng map shown in Figure 3-b is not much different from Figure 2-b. This means that the second polarization did not affect the playability much, at least for this particular note (D_3 at 147 Hz)

Longitudinal Bow-hair Vibration

To study the effect of the longitudinal bow-hair vibration, a one dimensional body effect and bow-hair vibration with rigid termination at frog and tip were included, while the dual polarization is turned off. Figure 4 shows the effective velocity of the bow-hair at the contact point. Although the nominal bowspeed was 0.05 m/s, the effective bowspeed fluctuates in the range of -0.15 m/s to 0.25 m/s. Thus, it is not surprising that Helmholtz motion could not be formed if forward slipping was not allowed. The dominant components of this velocity waveform are the fundamentals of the string (147 Hz) and the bow-hair in longitudinal direction (1770 Hz).
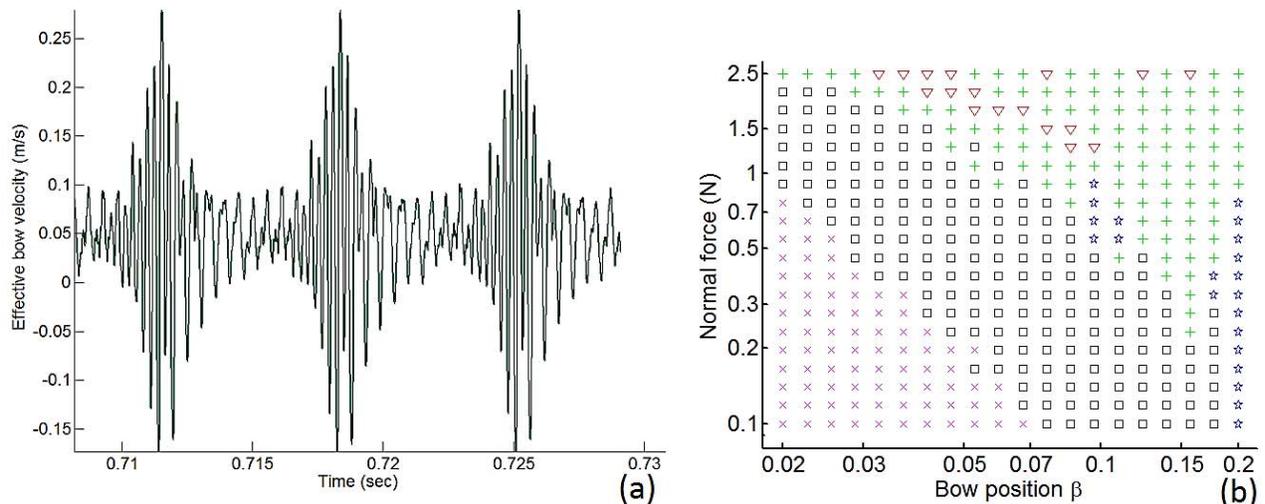

FIGURE 4: (a) time history of the effective bowspeed at the contact point. The nominal Bowspeed was 0.05 m/s and the simulation is made for Beta=0.02 and Bow-force=2.11 and the characteristic impedance of the bow-hair in longitudinal direction was 4.0 Ns/m (b) Schelleng diagram for the bowed string when longitudinal bow-hair vibration was allowed for.

Figure 4-b shows the Schelleng map constructed with this case. As was expected from the experience of players, the instrument played with an actual bow is more playable than the one bowed with a stick. Another interesting observation in Figure 4-b is the frequent occurrence of ALF compared to the case where longitudinal bow-hair vibration was not allowed. This point was emphasized by Mari Kimura in [Reel, 2009] *"The first secret is maintaining loose bow-hair…. You don't want a lot of tension… You need enough elasticity on the bow-hair that you can really grab the string."*

Stick Modes

Ultimately the combination of dual-string polarization, longitudinal bow-hair vibration and bow-stick modes were used in the model to produce the Schelleng diagram seen in Figure 5. The general shape of the diagram does not seem much different from Figure 4-b, which means most of the effect on the playability comes from the longitudinal bow-hair vibration rather than the string's second polarization or the stick modes. The playable range seems, however, a bit wider and the boundaries are better defined.
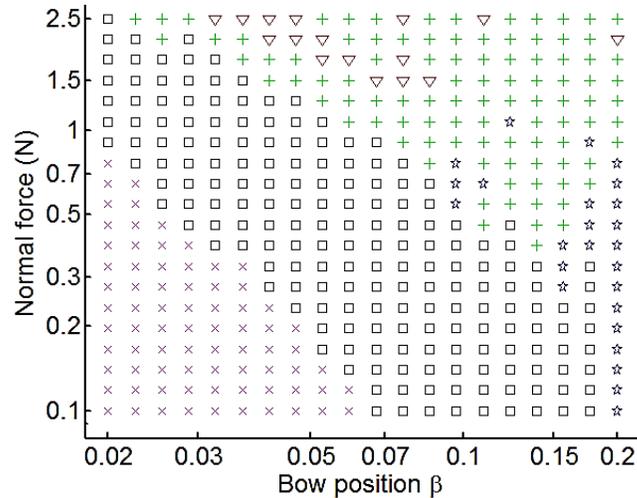
FIGURE 1: Schelleng diagram for the bowed string when longitudinal bow-hair vibration, stick modes, and dual string polarization are all taken into account

CONCLUSION

New features are added to the model of the bowed string for the first time. A detailed body model is implemented whose parameters were extracted from calibrated impedance measurements. The model takes into account the angle of body modes with respect to the bowing direction, which transforms the initial excitation of the string in the bowing direction to an excitation on the second polarization. A Schelleng diagram was produced that looks similar to ones found with simpler body models; however, our model reproduces the note-by-note variation of minimum bow-force. Secondly, inspired by our high-speed recordings of the bowed string, the second polarization of the string was taken into account by allowing the string to vibrate in both polarizations and the bow-hair to vibrate in its transverse direction. Although for the particular cello that we modeled the closest body mode to the fundamental of the string was almost parallel to the bowing direction, inclusion of the second polarization could still modulate the bow-force by 5.5%. Evidence is also provided for the second polarization to be strong enough to make an audible sound even in presence of the first string polarization. However, the Schelleng map of the open D string was not noticeably different when the second polarization was added. Finally the longitudinal vibration of the bow-hair was added to the model with and without the inclusion of the stick modes. It was seen that the longitudinal bow-hair vibration can modulate the effective bowspeed by more than 100% of its nominal value. The playable range of the instrument seems wider in the presence of the longitudinal bow-hair vibration and the occurrence of the ALF notes was much more frequent. The effect of the stick modes was definitely not as strong as the flexible bow-hair itself. In future studies the difference of the model with and without these details will be further studied and more details will be added to the model.

ACKNOWLEDGMENTS

REFERENCES

Askenfelt, A., **(1995)**, "Observations on the violin bow and the interaction with the string", Proceedings of the International Symposium on Musical Acoustics
Cremer L., **(1985)** "The physics of the violin". MIT Press, Cambridge MA,
Galluzzo, P., **(2003)**, "On the playability of stringed instruments", Ph. D. thesis, Trinity College, University of Cambridge, Cambridge, UK
Gough, C. **(1981)**, "The theory of string resonances on musical instruments", Acustica, 49, 124-141
Gough, C., **(2012)**, "Violin bow vibrations", The Journal of the Acoustical Society of America, 131, 4152

Pitteroff, R. and Woodhouse, J., **(1998a)** "Mechanics of the contact area between a violin bow and a string. Part I: Reflection and transmission behaviour," Acustica, Vol. 84, pp. 543–562.

Pitteroff, R. and Woodhouse, J., **(1998b)** "Mechanics of the contact area between a violin bow and a string. Part II: Simulating the bowed string," Acustica, Vol. 84, pp. 744–757.

Reel, J., **(2009)**, "Mari Kimura on Subharmonics", Strings, 107

Schelleng J. C., **(1973)**, "The bowed string and the player". J. Acoust. Soc. Am. 53, 26–41.

Schoonderwaldt, E.; Guettler, K. & Askenfelt, A. **(2008)** "An empirical investigation of bow-force limits in the Schelleng diagram", Acta Acustica united with Acustica, S. Hirzel Verlag, 94, 604-622

Schumacher, R., **(1975)**, "Some aspects of the bow," Catgut Acoust. Soc. Newsl. 24, 5–8.

Woodhouse, J. & Loach, A., **(1999)**, "Torsional behaviour of cello strings", Acta Acustica united with Acustica, S. Hirzel Verlag, 85, 734-740

Woodhouse, J. **(1993)**, "On the playability of violins. Part I: Reflection functions", Acustica, 78, 125-136

Woodhouse, J., **(2003)**, "Bowed string simulation using a thermal friction model", Acta Acustica united with Acustica, 89, 355-368

Woodhouse, J., **(2004)**, "On the synthesis of guitar plucks", Acta Acustica united with Acustica, S. Hirzel Verlag, 90, 928-944

Woodhouse, J. & Galluzzo, P. M., **(2004)**, "The bowed string as we know it today", Acta Acustica united with Acustica, 90, 579-589